DOI:10.11916/j.issn.1005-9113.19037

Simulated Sunlight Irradiation Based Photocatalytic Degradation of Acrylonitrile by Sn-F Co-doped TiO_2/SiO_2 Nano Powder Catalyst

Hanliang Li[1†], Shiyu Miao[2†], Lu Qiu[1], Bandna Bharti[1] and Feng Ouyang[1]*

(*1. School of Civil and Environmental Engineering, Harbin Institute of Technology, Shenzhen 518055, Guangdong, China;*
2. School of Life Science and Medicine, Dalian University of Technology, Panjin 124000, Liaoning, China)

Abstract: This study proved the significance of simulated sunlight irradiation response capability of Sn-F co-doped TiO_2/SiO_2 (Sn-F-TiO_2/SiO_2) photocatalysts, which were prepared by a simple sol-gel method and were evaluated by acrylonitrile degradation for photocatalytic activity. The synthesized catalysts were characterized by X-ray Diffraction (XRD), Scanning Electron Microscopy (SEM), Energy Dispersive Spectrometer (EDS), X-ray Photoelectron Spectroscopy (XPS), Brunauer-Emmett-Teller (BET), Ultraviolet-Visible Absorption spectroscopy (UV-Vis), and Photoluminescence Spectroscopy (PL). UV-Visible spectroscopy demonstrated that Sn doping caused remarkable red shift in TiO_2, which significantly increased the absorption efficiency of the catalysts. The XPS results showed that Sn was successfully doped into the TiO_2 lattice. The photocatalytic degradation of acrylonitrile indicated that the Sn-F-TiO_2/SiO_2 photocatalysts exhibited excellent photocatalytic activity when being annealed at 550 ℃ for 2 h. The degradation rate of acrylonitrile reached 67.7% after irradiation under simulated sunlight for 6 min, and the hole was the most important active species.

Keywords: photocatalysis; acrylonitrile degradation; Sn doping; F-TiO_2/SiO_2

CLC number: X506 **Document code**: A **Article ID**: 1005-9113(2021)01-0012-08

1 Introduction

Environmental conservation has attracted more and more social attention with the improvement of living standards, thus environment friendly treatment technology is strongly needed. Acrylonitrile is a kind of linear water-soluble polymer organic substance which is highly toxic and is suspected to be a human carcinogen. It can affect female fertility index, leading to embryo toxicity and abnormal musculoskeletal development, and it may also cause great toxicity to organism when being discharged into the environment[1]. As an important industrial raw material, acrylonitrile has unparalleled function in chemical industry that although the production of acrylonitrile has met the market demand and brought certain economic benefits, it poses a challenge to environmental protection[2-4].

Since the traditional removal methods for acrylonitrile have the drawbacks of high cost, insufficient removal ratio, and rigid reaction conditions, a new removal method is urgently needed. In recent years, photocatalytic technology has developed rapidly and many studies have been conducted on photocatalytic hydrogen production[5-6], photoelectrocatalysis[7-10], and photocatalytic degradation. Various mature catalyst modification methods have also been applied, including template method[11], core-shell structure[12], and quantum dot modification[13]. Photocatalytic degradation provides a novel idea and is a simple approach for acrylonitrile decomposition, which exhibits the advantages of low cost, reaction at easy control condition, non-toxicity, and good chemical stability[14].

For most organic and inorganic substances, titanium dioxide (TiO_2) photocatalyst can completely oxidize target substances into water, carbon dioxide, inorganic acid, and other low molecular substances which are not harmful to the environment. However,

Received 2019-04-25.
Sponsored by the Science and Technology Commission of Shenzhen Municipality, P. R. China (Grant Nos. JCYJ20140417172417138 and ZDSYS20140508161622508).
†These authors contributed equally to this work.
* Corresponding author. E-mail: ouyangfh@hit.edu.cn.

the relatively large electronic band gap of TiO_2 limits its photoresponse to solar irradiation. Besides, the fast recombination of electron-hole pairs reduces the quantum conversion efficiency of TiO_2[15], which suggests the major drawback of photocatalytic activity. Therefore, considerable efforts have been made to promote photocatalytic activity by several modifications.

In our previous studies, thephotocatalytic activity had been promoted by F doping (F-TiO_2/SiO_2). Meanwhile, SiO_2 which acts as a carrier can increase the surface area[16]. For the purpose of further improving the efficiency of the catalyst, scientists have explored different technics to broaden the spectral absorption region of titanium oxide, among which metal ion doping is a promising method.

Metal ion doping can introduce defect position in semiconductor lattice or change the crystallinity of the semiconductor, thus affecting the electron-hole pair recombination[17-19]. Among these metals, Sn and Ti have similar ionic radii (r_{SnIV} = 0.69 Å, r_{TiIV} = 0.61 Å)[20], which makes Sn well doped into the TiO_2 lattice. The present study explored the influences of Sn doping and annealing process on catalyst surface structure. Effects of Sn doping and annealing process on the acrylonitrile degradation were also estimated, and the active species for oxidation were investigated by adding sacrificial agents.

2 Materials and Methods

2.1 Materials

Ethanol (CH_3CH_2OH, AR), ice acetic acid (CH_3COOH, AR), hydrofluoric acid (HF, AR), isopropyl alcohol (IPA, AR), ethylenediamine tetraacetic acid (EDTA, AR), tetrabutyl titanate (TBT, AR), silica gel ($mSiO_2 \cdot H_2O$, 100 ~ 200 mesh), stannic chloride pentahydrate ($SnCl_4 \cdot 5H_2O$, AR), p-benzoquinone (BQ, AR), and acrylonitrile (C_3H_3N, AR) were used for the experiment.

2.2 Catalyst Preparation

Sol-gel method was applied to prepare the catalysts in this study. The preparation steps are as follows. First, 5 mL TBT was added to 13 mL ethanol at room temperature, which was then stirred vigorously to form solution *A*. Next, 21 mL ethanol, 4 mL glacial acetic acid, 0.7 mL hydrofluoric acid, and 1.05 mL water were mixed with a certain concentration of $SnCl_4$ for the molar rate of Sn : Ti to be 0.01 : 1 to form uniform and transparent solution *B*. After being stirred for 20 min, solution *B* was slowly added to solution *A*, which was then added with suitable amount of silica gel (SiO_2 carrier). The obtained solution was stirred until gel was formed, and Sn-F-TiO_2/SiO_2 was formed by aging the gel at 25 ℃ and then dried. Sn-F-TiO_2/SiO_2 nanoparticles were obtained by annealing gel powders in air at different temperatures from 350 ℃ to 750 ℃. TiO_2/SiO_2, F-TiO_2/SiO_2, and Sn-TiO_2/SiO_2 were prepared by the sol-gel method as described in previous study[16].

2.3 Evaluation of Photocatalytic Activity

A cylindrical quartz reactor with 100 mm height and 60 mm inner diameter was used for the experiment. 150 mg photocatalyst powders were dispersed in 150 mL acrylonitrile solution (10 mg/L). The suspension was stirred in dark for 30 min to reach adsorption equilibrium, and then a spherical xenon lamp (350 w, Shenzhen An Hong Da Opto Technology Co., Ltd.) was used as simulated sunlight source, which was placed with a distance of 100 mm above the reactor.

The photocatalytic degradation of the acrylonitrile solution was performed in a batch experiment. The concentration of the acrylonitrile in the solution was determined by High Performance Liquid Chromatography (HPLC, Model: Tian Mei LC2000, China; Column: SHIMADZU-GL Wonda Cract ODS-2). The mobile phase was a mixture of deionized water and methanol (7 : 3 V/V) with the flow rate of 1.0 mL/min and the detection wavelength of 210 nm. The retention time for acrylonitrile was 7.24 min. The removal of acrylonitrile was determined by

$$\text{Removal}(\%) = (C_0 - C_t)/C_0 \times 100\% \quad (1)$$

where C_0 and C_t are the concentrations of acrylonitrile before and after the photocatalytic reaction respectively.

2.4 Catalyst Characterizations

X-ray Diffraction (XRD) patterns were obtained on a Rigaku D/max 2500 PC diffractometer with Cu Kα radiation (λ = 1.54056 Å) at a tube current of 20 mA and a voltage of 40 kV. X-ray Photoelectron Spectroscopy (XPS) was measured on a Thermo ESCALAB 250XI instrument with Al Kα X-ray source (h_ν = 1486.6 eV). All binding energies were calibrated to the C1s peak of the instrument at 284.62 eV. Scanning Electron Microscopy (SEM) and Energy Dispersive Spectrometer (EDS) images

were obtained by HITACHI SU8010. Photoluminescence Spectroscopy (PL) spectra were determined by an SHIMADZU RF5301PC using 380 nm line of an Xe lamp as the excitation source. Brunauer-Emmett-Teller (BET) specific surface area of the catalysts was obtained using a Belsorp-mini nitrogen gas adsorption instrument.

3 Results and Discussion

3.1 XRD Analysis

Sn-F-TiO_2/SiO_2 catalysts were annealed at different temperatures to verify the optimal preparation conditions. The molar ratio of Sn : F was 0.01 : 1 and the annealing time was 2 h. Fig.1(a) shows the XRD patterns of the catalysts annealed from 350 ℃ to 750 ℃, and the results indicate that the samples had the same distinctive peaks with varying temperature. The characteristic peaks at 2θ = 25.26°, 37.86°, 48.08°, 53.86°, 55.09°, 62.82°, 68.93°, 70.28°, and 75.10° corresponded to the anatase crystal planes (JCPDS 21-1272), which shows that there was no phase transition from anatase phase to rutile phase at 350－750 ℃. No peaks of Sn or SnO_2 phases were observed for the low doping concentration of Sn. With increasing annealing temperature, the diffraction peaks gradually narrowed, indicating the increase of the corresponding crystallinity. Crystal sizes of Sn-F-TiO_2/SiO_2 particles were calculated with Scherrer equation[16].

The specific surface area and crystal sizes at different annealing temperature ranges are shown in Table 1.

The photocatalytic activities of the Sn-F-TiO_2/SiO_2 catalysts with different annealing temperatures for acrylonitrile degradation under simulated sunlight within 6 min were tested and the results are presented in Fig.1(b). It can be found that with the increase of the annealing temperature from 350 ℃ to 550 ℃, the degradation rate of acrylonitrile increased from 36.1% to 67.7%, while as the temperature rose further, the photocatalytic degradation rate decreased to 47.59%, which is attribute to the increase of the catalyst crystallinity and the decrease of the specific surface area (Table 1). Owing to the reduction in the specific surface area, hole density was decreased on the surface of the catalyst, which also resulted in the less electron-hole recombination and thus improved the catalyst activity. However, further increase in the temperature may lead to the agglomeration of the catalysts and therefore decreased the photocatalytic activity.

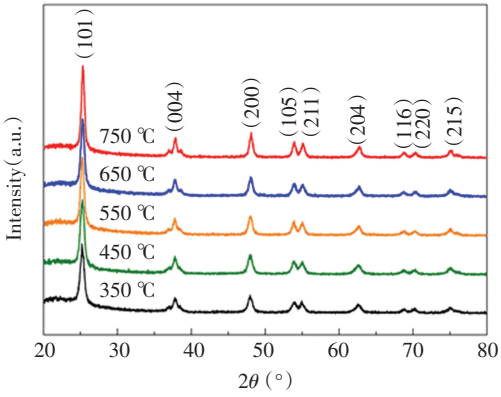

(a) XRD patterns of Sn-F-TiO_2/SiO_2 catalysts prepared from 350 ℃ to 750 ℃

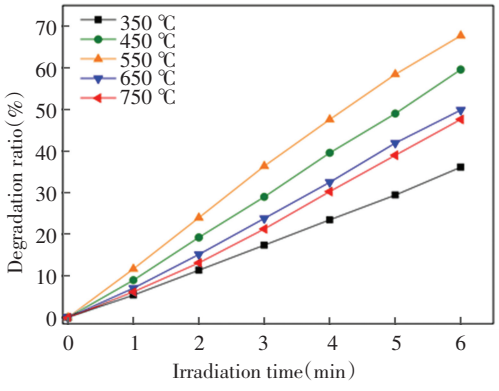

(b) Influence of annealing temperature on the activity of Sn-F-TiO_2/SiO_2 catalysts

Fig.1 Influence of temperature on crystal structure and photocatalytic activity of Sn-F-TiO_2/SiO_2 catalysts

Table 1 Specific surface area and crystal size of Sn-F-TiO_2/SiO_2 catalysts from 350 ℃ to 750 ℃

Annealing temperatures(℃)	Specific surface area (m^2/g)	Crystal size (nm)
350	221	12.3
450	220	15.7
550	218	15.3
650	216	17.1
750	210	19.5

3.2 Surface Morphology of the Catalysts

To clarify the effect of Sn doping on the surface morphology of the catalysts, SEM and EDS images of the catalysts including TiO_2/SiO_2, F-TiO_2/SiO_2, and Sn-F-TiO_2/SiO_2 were obtained as presented in Fig.2.

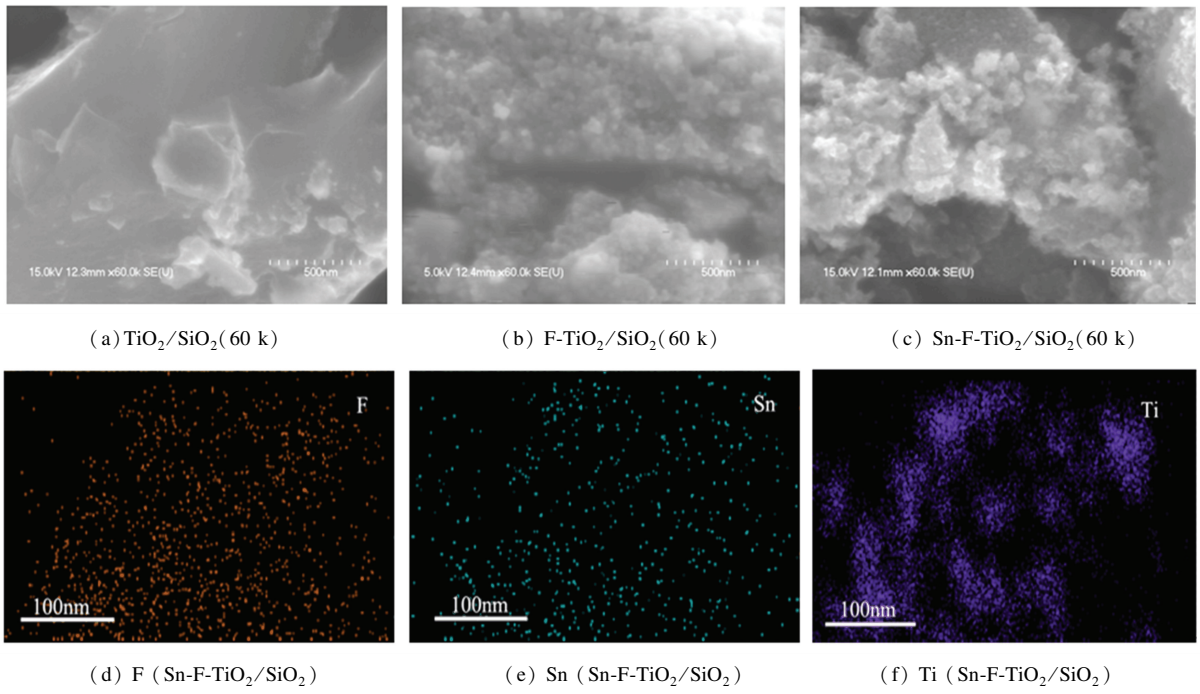

(a) TiO_2/SiO_2 (60 k) (b) F-TiO_2/SiO_2 (60 k) (c) Sn-F-TiO_2/SiO_2 (60 k)

(d) F (Sn-F-TiO_2/SiO_2) (e) Sn (Sn-F-TiO_2/SiO_2) (f) Ti (Sn-F-TiO_2/SiO_2)

Fig.2 SEM images of TiO_2/SiO_2, F-TiO_2/SiO_2, and Sn-F-TiO_2/SiO_2 catalysts as well as EDS images of Sn-F-TiO_2/SiO_2 catalysts

SEM images showed that TiO_2/SiO_2, F-TiO_2/SiO_2, and Sn-F-TiO_2/SiO_2 catalysts were secondary particles formed by the irregular accumulation of primary particles. Sn doping had no obvious effect on the grain morphology and the aggregation of F-TiO_2/SiO_2 samples. Compared with TiO_2/SiO_2 catalyst, F-TiO_2/SiO_2 catalyst possessed a large number of tiny grains on the surface, which might be due to the corrosion of hydrogen fluoride on the surface of the sample. In the process of sample preparation, the presence of fluoride ions could loosen the surface of the nanocrystals and reduce the bulk density of the samples. After doping Sn into F-TiO_2/SiO_2 catalyst, the morphology had no obvious difference with the F-TiO_2/SiO_2 catalyst, implying that Sn doping did not influence the rough surface structure. EDS images showed that F, Sn, and Ti elements were evenly distributed in Sn-F-TiO_2/SiO_2 catalysts.

3.3 PL Study

For semiconductor nanomaterial, the PL spectra were related to the transmission behavior of photogenerated electron-hole pairs. Fig. 3 illustrates the PL spectra of different catalysts. The PL spectra of F-TiO_2/SiO_2 catalyst samples showed several strong emission peaks in the range of 350 nm to 550 nm. When Sn was doped, the peak emission intensity decreased to a small extent, which indicates that Sn doping inhibited the recombination of photo-induced electrons and holes, thus improving the activity of the catalysts[21].

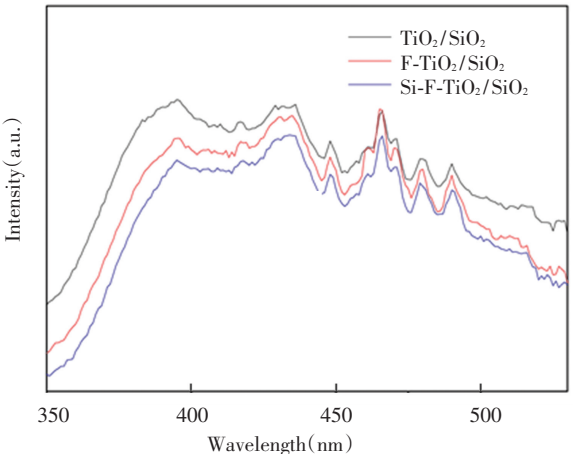

Fig.3 PL spectra of TiO_2/SiO_2, F-TiO_2/SiO_2, and Sn-F-TiO_2/SiO_2 catalysts

3.4 XPS Analysis

The surface composition and the valence state of the elements in the catalysts were determined by XPS. Fig.4(a) shows the XPS survey spectra, in which all added elements can be observed. In Fig.4(b), F 1s had two peaks positions, which suggests that F

existed in two different states. The binding energy located at 687.8 eV was caused by the substitution of F atoms for the position of oxygen atoms in the TiO_2 lattice[22]. It reveals that the preparation of catalyst samples by the sol-gel method with HF as the precursor could enable F atoms to enter the lattice of TiO_2. The binding energy located at 684.7 eV was due to the adsorption of F ions on the TiO_2 surface[15], which implies that Sn doping had no effect on the state of adsorption for F ions. Fig.4(c) presents the O 1s spectra of Sn-F-TiO_2/SiO_2, where the peaks were at binding energies 529.9 eV and 533.4 eV, indicating that there were at least two chemical states of oxygen. The peak near the position of 533.4 eV belonged to the oxygen in the hydroxyl groups (·OH)[23], suggesting the existence of hydroxyl ions on the sample surface. These ·OH ions are important species for photocatalysis. The peak near the position of 529.9 eV belonged to the oxygen in the TiO_2 lattice[24]. Fig.4(d) shows Sn 3d peaks at two positions of binding energies (486.4 eV and 495.0 eV), and the cause was the tetravalent tin ions into the lattice of TiO_2[25], which indicates that Sn was successfully doped into the TiO_2 lattice.

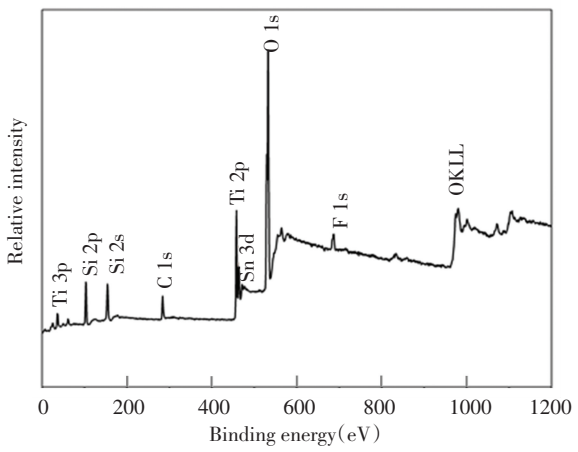

(a) XPS survey spectra

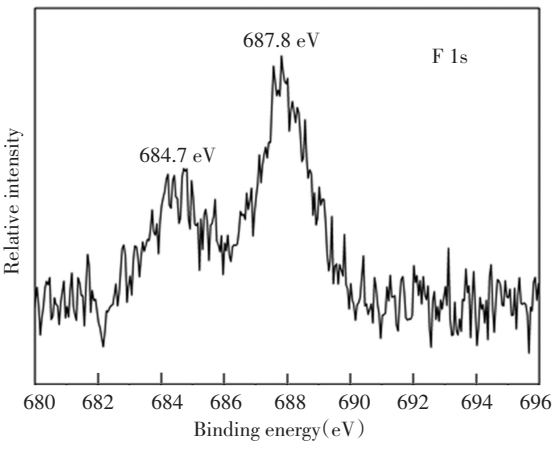

(b) F 1s

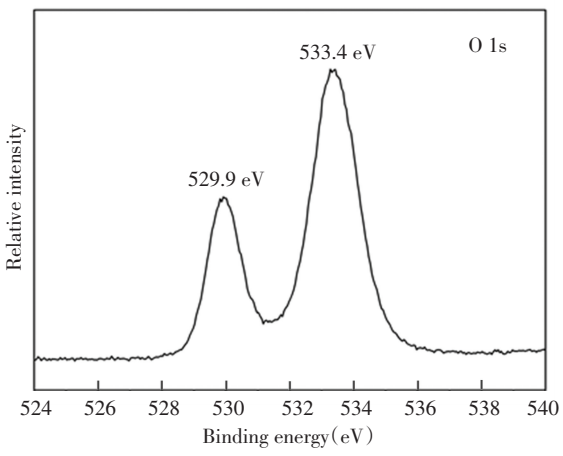

(c) O 1s

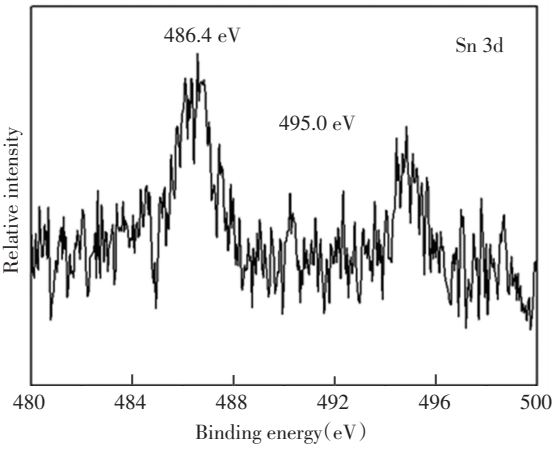

(d) Sn 3d

Fig.4 XPS survey spectra and high resolution XPS spectra of Sn-F-TiO_2/SiO_2 catalyst

3.5 Ultraviolet-Visible Absorption Spectroscopy (UV-Vis) Analysis

The light absorption of the catalysts before and after Sn doping was investigated by UV-Visible spectra. As shown in Fig.5, the absorption edge of the Sn-F-TiO_2/SiO_2 catalyst shifted a little toward longer wavelength compared with the F-TiO_2/SiO_2 catalyst samples. In particular, the absorption of light was obviously enhanced from 380 nm, indicating that Sn doping could expand the optical adsorption performance of F-TiO_2/SiO_2 catalysts and then improve the absorption efficiency of the catalysts to light.

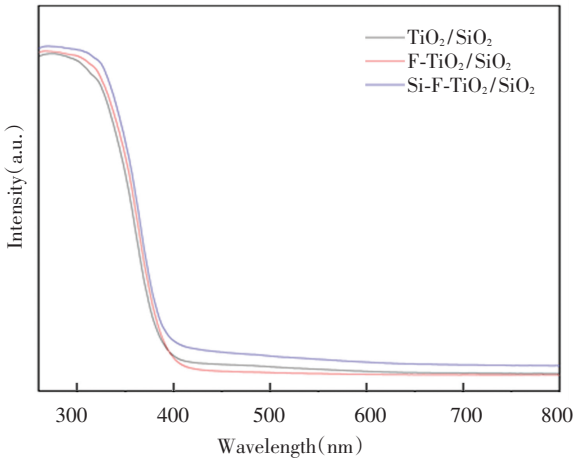

Fig.5 UV-Vis absorption spectra of TiO_2/SiO_2, F-TiO_2/SiO_2, and Sn-F-TiO_2/SiO_2 catalysts

3.6 Photocatalytic Activity

The photocatalytic activities of Sn-F-TiO_2/SiO_2 catalysts were evaluated by acrylonitrile degradation under simulated sunlight. Fig.6 shows the degradation efficiency of acrylonitrile with TiO_2/SiO_2, F-TiO_2/SiO_2, and Sn-F-TiO_2/SiO_2 photocatalyst samples. As shown in Fig.6, the degradation rate of acrylonitrile reached 67.7% after irradiated under simulated sunlight for 6 min with Sn-F-TiO_2/SiO_2 catalyst. Apparently, this degradation efficiency was higher than F-TiO_2/SiO_2 and TiO_2/SiO_2, and the result was consistent with those of UV-Visible and PL spectra.

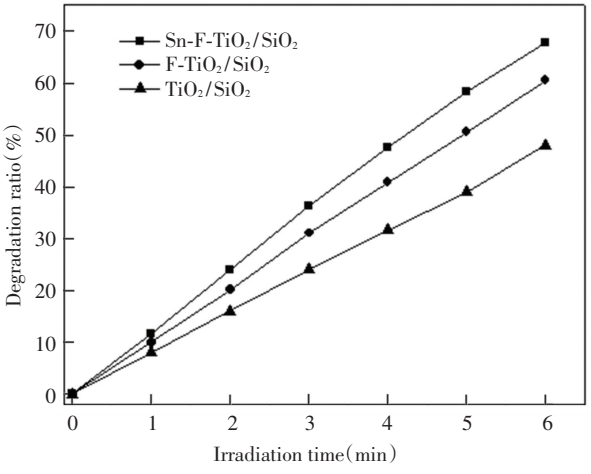

Fig.6 Degradation efficiency of acrylonitrile with TiO_2/SiO_2, F-TiO_2/SiO_2, and Sn-F-TiO_2/SiO_2 catalyst samples

Furthermore, the photocatalytic degradation of acrylonitrile was first-order kinetically fitted (as shown in Table 2). The linear correlation coefficients R^2 of the three catalysts in the reaction systems were 99.9%, 99.9%, and 99.8%, respectively, indicating that the photocatalytic reaction conformed to be the first-order reaction kinetics model. Compared with 7.90 min^{-1} (TiO_2/SiO_2 catalyst), the apparent rate constant increased from 10.12 min^{-1} (F-TiO_2/SiO_2 catalyst) to 11.44 min^{-1} (Sn-F-TiO_2/SiO_2 catalyst), which indicates that Sn doping could further improve the reaction rate.

Table 2 Apparent rate constants and correlation coefficients for the first-order kinetics of photocatalytic degradation of acrylonitrile

Photocatalysts	Apparent rate constants (min^{-1})	Correlation coefficients (R^2)
TiO_2/SiO_2	7.90	0.999
F-TiO_2/SiO_2	10.12	0.999
Sn-F-TiO_2/SiO_2	11.44	0.998

3.7 Stability of Sn-F-TiO_2/SiO_2

After five replicate experiments, the catalysts maintained good photocatalytic efficiency, which means that Sn-F co-doped samples were relatively stable and could remain high efficiency in photodegradation under simulated sunlight irradiation (as shown in Fig.7).

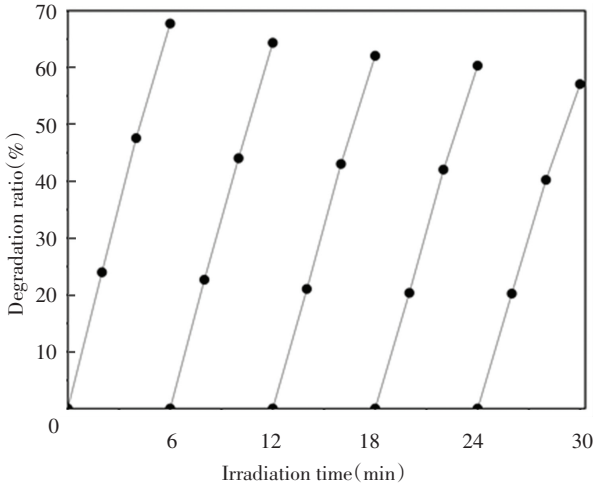

Fig.7 Recycle efficiency of Sn-F-TiO_2/SiO_2 catalyst samples under simulated sunlight

4 Investigation of Active Species

During the photocatalytic reaction, the active species of oxidation mainly included hydroxyl radicals (·OH), hole (h^+), and superoxide anion ($O_2 \cdot^-$). Sacrificial agents were added to distinguish the activity of oxidative species during the

photocatalytic degradation of acrylonitrile, consisting of IPA for ·OH, EDTA for h^+, and BQ for $O_2 \cdot^-$. Fig.8 demonstrates the photocatalytic degradation of acrylonitrile by Sn-F-TiO_2/SiO_2 under simulated sunlight through adding different sacrificial agents. Results reveal that the use of three different sacrificial agents led to the decline of the photocatalytic degradation activity to a certain extent, indicating that the corresponding ·OH, h^+, and $O_2 \cdot^-$ were related to the photodegradation process. When IPA, EDTA, and BQ were added, the photocatalytic activity decreased, and the removal rates of acrylonitrile were 38.17%, 1.90%, and 14.80%, respectively. It implies that the hole was the most active species during the photodegradation of acrylonitrile. Usually, hydroxyl radicals are crucial during the photodegradation of pollutants, while they mainly extract and add hydrogen atoms in carbon-hydrogen bonds to decompose pollutants[26]. However, in the absence of carbon-hydrogen bonds, holes play a major role in oxidation[27].

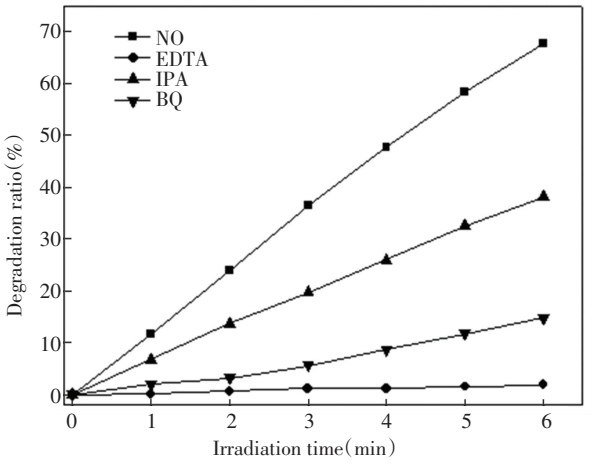

Fig.8 Effects of different sacrificial agents on the photodegradation activity of acrylonitrile by Sn-F-TiO_2/SiO_2 catalysts

Acrylonitrile contains a carbon-nitrogen triple bond, wherein the bond is very strong, so the degradation of acrylonitrile is mainly dependent on the holes. According to Fig.8, it can be found that ·OH and $O_2 \cdot^-$ played auxiliary roles.

5 Conclusions

Sn-F-TiO_2/SiO_2 catalysts were prepared by a sol-gel method. Acrylonitrile was degraded under simulated sunlight to evaluate photocatalytic activities. The activity of Sn-F-TiO_2/SiO_2 catalyst for acrylonitrile degradation was systematically investigated. Improved by Sn doping, Sn-F-TiO_2/SiO_2 catalysts showed 67.7% degradation of acrylonitrile. Characterization results indicated that compared with F-TiO_2/SiO_2, Sn-F-TiO_2/SiO_2 catalysts had smaller crystal size, smaller grain surface, and looser granules, which was in favor of even dispersion of the catalyst powders in the reaction systems. PL was also slightly weakened, which implied the inhibited recombination of photo-induced electrons and holes. Red shift of absorption edge occurred and thus the utilization rate of light was higher, which enhanced the photocatalytic activity. The XPS results indicated that Sn was successfully doped into the lattice of the catalysts. Addition of sacrificial agents into the reaction systems showed that the hole was the most important active species for the photocatalytic activity.

References

[1] Poushali B, Tushar K D, Sayan G, et al. Selective cross-linking of carboxylated acrylonitrile butadiene rubber and study of their technological compatibility with poly (ethylene-co-methyl acrlylate) by means of mechanical, thermal, and chemical analysis. Polymer Bulletin, 2019, 76(4): 1877-1897. DOI: 10.1007/s00289-018-2474-z.

[2] Lu Y Y, Xu N K, Lv Y Y, et al. Fibrous material based on a combination of poly(acrylic acid-co- hydroxyethyl methacrylate) with iron ions as a heterogeneous Fenton catalyst for dye oxidative decomposition. Journal of Applied Ploymer Science, 2017, 134(27): 44875. DOI: 10.1002/app.44875.

[3] Léonard A, Gerber G B, Stecca C, et al. Mutagenicity, carcinogenicity, and teratogenicity of acrylonitrile. Mutation Research/Reviews in Mutation Research, 1999, 436(3): 263-283. DOI: 10.1016/S1383-5742(99)00006-X.

[4] Jõks S, Krichevskaya M, Preis S. Gas-phase photocatalytic oxidation of acrylonitrile on sulphated TiO_2: Continuous flow and transient study. Catalysis Letters, 2011, 141(2): 309-315. DOI: 10.1007/s10562-010-0501-2.

[5] Li L, Salvador P A, Rohrer G S. Photocatalysts with internal electric fields. Nanoscale, 2014, 6(1): 24-42. DOI: 10.1039/c3nr03998f.

[6] Wang L J, Wang W Z, Chen Y L, et al. Heterogeneous *p-n* junction CdS/Cu_2O nanorod arrays: Synthesis and superior visible-light-driven photoelectrochemical performance for hydrogen evolution. ACS Applied Materials & Interfaces, 2018, 10(14): 11652-11662. DOI: 10.1021/acsami.7b19530.

[7] Wang H, Liu X, Wang S L, et al. Dual templating

fabrication of hierarchical porous three-dimensional ZnO/carbon nanocomposites for enhanced photocatalytic and photoelectrochemical activity. Applied Catalysis B: Environmental, 2018, 222: 209-218. DOI: 10.1016/j.apcatb.2017.10.012.

[8] Wang H, Liu H, Wang S L, et al. Influence of tunable pore size on photocatalytic and photoelectrochemical performances of hierarchical porous TiO_2/C nanocomposites synthesized via dual-Templating. Applied Catalysis B: Environmental, 2018, 224: 341-349. DOI: 10.1016/ j.apcatb.2017.10.039.

[9] Xu T T, Liu X, Wang S L, et al. Ferroelectric oxide nanocomposites with trimodal pore structure for high photocatalytic performance. Nano-Micro Letters, 2019, 11(1): 37. DOI: 10.1007/s40820-019- 0268-y.

[10] Xu T T, Wang S L, Li L, et al. Dual templated synthesis of tri-modal porous $SrTiO_3/TiO_2$ @ carbon composites with enhanced photocatalytic activity. Applied Catalysis A: General, 2019, 575: 132 - 141. DOI: 10.1016/j.apcata.2019.02.017.

[11] Chen Y L, Wang L J, Wang W Z, et al. Enhanced photoelectrochemical properties of ZnO/ZnSe/CdSe/Cu_{2-x}Se core-shell nanowire arrays fabricated by ion-replacement method. Applied Catalysis B: Environmental, 2017, 209: 110-117. DOI: 10.1016/j.apcatb.2017.02.049.

[12] Chen Y L, Wang L J, Wang W Z, et al. Synthesis of Se-doped ZnO nanoplates with enhanced photoelectrochemical and photocatalytic properties. Materials Chemistry and Physics, 2017, 199: 416 - 423. DOI: 10.1016/j.matchemphys.2017.07.036.

[13] Wang L J, Wang W Z, Zhang WW, et al. Superior photoelectrochemical properties of $BiVO_4$ nanofilms enhanced by PbS quantum dots decoration. Applied Surface Science, 2018, 427(Part B): 553-560. DOI: 10.1016/j.apsusc.2017.09.014.

[14] Dai Y, Song Y, Tu X, et al. Sequential shape-selective adsorption and photocatalytic transformation of acrylonitrile production wastewater. Water Research, 2015, 85(3): 216-225. DOI: 10.1016/j.watres.2015.08.034.

[15] Wu Y, Xing M, Tian B, et al. Preparation of nitrogen and fluorine co-doped mesoporous TiO_2 microsphere and photodegradation of acid orange 7 under visible light. Chemical Engineering Journal, 2010, 162(2): 710-717. DOI: 10.1016/j.cej.2010.06.030.

[16] Pang D D, Wang Y T, Ma X D, et al. Fluorine promoted and silica supported TiO_2 for photocatalytic decomposition of acrylonitrile under simulant solar light irradiation. Chemical Engineering Journal, 2014, 258: 43-50. DOI: 10.1016/j.cej.2014.07.068.

[17] Zheng S K, Wu G H, Zhang J Y, et al. Energy band structure and photocatalytic activity of Sn-doped TiO_2 thin films. Journal of Materials Engineering, 2014, (1): 70-74. DOI: 10.3969/j.issn.1001-4381.2014.01.013. (in Chinese)

[18] Kyeremateng N A, Vacandio F, Sougrati M T, et al. Effect of Sn-doping on the electrochemical behaviour of TiO_2 nanotubes as potential negative electrode materials for 3D Li-ion micro batteries. Journal of Power Sources, 2013, 224: 269-277. DOI: 10.1016/j.jpowsour.2012.09.104.

[19] Zheng S K, Wang T M, Hao W C, et al. Improvement of photocatalytic activity of TiO_2 thin film by Sn ion implantation. Vacuum, 2002, 65(2): 155-159. DOI: 10.1016/s0042-207x(01)00424-9.

[20] Duan Y D, Zheng J X, Ming X, et al. Metal and F dual-doping to synchronously improve electron transport rate and lifetime for TiO_2 photoanode to enhance dye-sensitized solar cells performances. Journal of Materials Chemistry A, 2015, 3(10): 5692-5700. DOI: 10.1039/c4ta07068b.

[21] Xiang Q J, Lv K L, Yu J G. Pivotal role of fluorine in enhanced photocatalytic activity of anatase TiO_2 nanosheets with dominant (0 0 1) facets for the photocatalytic degradation of acetone in air. Applied Catalysis B: Environmental, 2010, 96(3-4): 557-564. DOI: 10.1016/j.apcatb.2010.03.020.

[22] Lv L, Bai X, Ye Z. Construction of N-doped TiO_2/SnO_2 heterostructured microspheres with dominant {001} facets for enhanced photocatalytic properties. CrystEngComm, 2016, 18(39): 7580-7589. DOI: 10.1039/C6CE01209D.

[23] Yang G, Jiang Z, Shi H, et al. Study on the photocatalysis of F-S co-doped TiO_2 prepared using solvothermal method. Applied Catalysis B: Environmental, 2010, 96(3-4): 458-465. DOI: 10.1016/j.apcatb.2010.03.004.

[24] Reddy P A K, Srinivas B, Kala P, et al. Preparation and characterization of Bi-doped TiO_2 and its solar photocatalytic activity for the degradation of isoproturon herbicide. Materials Research Bulletin, 2011, 46(11): 1766-1771. DOI: 10.1016/ j.materresbull.2011.08.006.

[25] Zhu X J, Guo Z P, Zhang P, et al. Three-dimensional reticular tin-manganese oxide composite anode materials for lithium ion batteries. Electrochimica Acta, 2010, 55(17): 4982-4986. DOI: 10.1016/j.electacta.2010.03.107.

[26] Jaeger C D, Bard A J. Spin trapping and electron spin resonance detection of radical intermediates in the photodecomposition of water at titanium dioxide particulate systems. Journal of Physical Chemistry, 1979, 83(24): 3146-3152. DOI: 10.1021/j100487a 017.

[27] Mao Y, Schoeneich C, Asmus K D. ChemInform Abstract: Identification of organic acids and other intermediates in oxidative degradation of chlorinated ethanes on TiO_2 surfaces en route to mineralization. A combined photocatalytic and radiation chemical study. ChemInform, 2010, 95(24): 10080-10089. DOI: 10.1002/chin.199210088.